September 2023, Vol:1, No:1

International Journal of New Findings in Engineering, Science and Technology

journal homepage: *https://ijonfest.gedik.edu.tr/*

Design of a Cold Storage with R507A Refrigerant for the Preservation of Twenty-Five Tons of Apples in the Ankara Province

Berker Özün Fenni[a], Ali Köse[b*], Parisa Heidarnejad[c]

[a]*B.Sc. in Mechanical Engineering, Türkiye, berker.ozun@hotmail.com*
[b]*Research Assistant, , Faculty of Engineering, Department of Mechanical Engineering, Istanbul Gedik University, Türkiye, ali.kose@gedik.edu.tr(*Corresponding Author)*
[c]*Assistant Professor, Faculty of Engineering, Department of Mechanical Engineering, Istanbul Gedik University, Türkiye parisa.heidarnejad@gedik.edu.tr*

Abstract

In the absence of proper humidity and temperature conditions, undried fresh foods will experience physiological and biological deterioration, resulting in mass loss and the development of mold. Thanks to this rationale, humanity has endeavored to keep food products from deteriorating. This can be observed through the use of cold rooms constructed by the Ancient Romans using clay and the cooling chambers known as "Yakhchāl" developed by the Persians. The advancement of refrigeration technology has persisted since the era of ancient civilizations. The advent of refrigeration cycles has significantly streamlined the implementation of containment technology. The presence of these systems in residential settings can be attributed to the development of the vapor compression refrigeration cycle and the compact nature of this technology, which enables convenient freezing or cooling of products for storage purposes. Vapor compression refrigeration cycles are still widely employed in various applications, such as office and automotive air conditioning systems, refrigerators, and industrial cold rooms. This study aims to develop an industrial cold room design tailored explicitly for storing and transporting apples, a perishable agricultural commodity. The primary objective is to ensure that the apples are maintained in optimal humidity and temperature conditions, thereby preventing any degradation, even when handling large quantities in Ankara.

Keywords: Refrigerant; Cold storage; Vapor compression cycle; Refrigeration; Fresh food

1. INTRODUCTION

The cooling process is commonly referred to as a closed cycle, wherein heat is transferred from the surrounding environment to a different location using a refrigerant [1]. The vapor compression refrigeration cycle is used to lower the temperature of a medium through the cooling process resulting from the phase transition of the refrigerant.

Throughout history, humanity has employed diverse methodologies dating back to ancient civilizations in order to preserve and extend the shelf life of food. Architectural remnants attributed to ancient civilizations, including the Greeks, Romans, Sumerians, and Persians, are extant. One notable illustration of such architectural structures is represented by the Yakhchāls, which the ancient Persians ingeniously constructed for passive cooling and food preservation. These structures are outfitted with walls that possess a dome-shaped configuration and are constructed using a combination of clay and diverse composite materials. Additionally, these structures are equipped with channels that are interconnected to a nearby water source and propellers that facilitate air circulation within the interior.

In 1916, the DOMELRE company introduced an affordable, lightweight, and compact electric refrigerator to the consumer market. During that period, certain refrigerants, namely ammonia (R717), chloromethane (R40), and sulfur dioxide (R764), were used due to a lack of awareness regarding their detrimental effects on the environment [1-3]. The development of the initial chlorofluorocarbon, R-12, which was less harmful to the environment, occurred in 1928 thanks to progress in chemical technology [4]. Following that, two professors with ties to the University of California elaborated on the detrimental effects of chlorinated halocarbons on the ozone layer in a 1974 article. As a result, the Montreal Protocol Agreement, enacted in 1984, banned the utilization of these chlorofluorocarbons (CFCs).

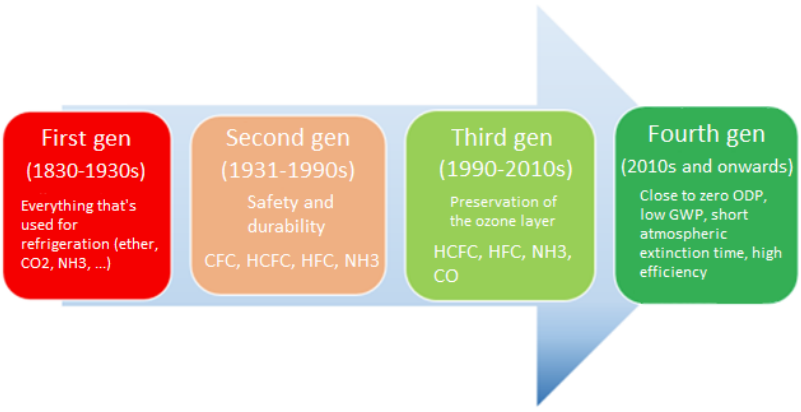

Figure 1. Historical development of refrigerants [5]

In Figure 1, the development of refrigerants throughout history can be seen. Historically, refrigerants incorporating fluorine and ammonia were employed for some time, unknowingly of their detrimental effects on the environment. Consequently, in 1996, a transition was made to hydrofluorocarbon (HFC) based refrigerants [6]. Currently, the most commonly employed refrigerants in industrial and domestic refrigeration systems are R134A, R32, and R125. The refrigerants mentioned in this context have been developed to mitigate the adverse effects of global warming potential (GWP) and ozone depletion potential (ODP) [7].

1.1. *Related Literature*

A variety of insulation and construction materials have been utilized in the current set of literature, engineered projects, and constructed cold rooms. Each food product has specific storage conditions.

The study, carried out by Koyuncu and Eren [8], involved procuring Granny Smith, Imparatore, and Idared apple cultivars from orchards established with M9 rootstock at the Eğirdir Horticultural Research Institute. The experiment was conducted at the Post-Harvest Physiology Laboratory, which is in the Department of Horticulture within the Faculty of Agriculture at Süleyman Demirel University in Isparta.

The cold room was consistently maintained at a relative humidity level of 90 % to 95 %. Specimens exhibiting physiological deterioration were subjected to a separation process with a one-month interval between each instance. In the initial year study, various apple cultivars, namely Granny Smith, Imparatore, and Idared, experienced mass losses of 0.7 %, 1.19 %, and 0.95 %, respectively, when stored at 0°C for six months. In the second year of the study, the average mass losses of the apples, which underwent a storage period of 6 months at three distinct temperatures (-1°C, 0°C, and 2°C), were observed to be as follows: 1.57–1.7 % for Granny Smith, 1.77 %-2.22 % for Imparatore, and 2.38 %-3.51 % for Idared. Based on the results of this study, the apples stored at a temperature of 0°C exhibited the lowest degree of mass.

According to West and Kedd [9], recent advancements in gas storage technology present a viable alternative to traditional cool rooms for storing apples and pears. Based on the findings of West and Kedd, subjecting apples to a temperature of 1°C resulted in the manifestation of a disease known as "low-temperature breakdown." This condition is characterized by the deceptive appearance of normalcy in the apples, despite their rapid deterioration during the subsequent distribution process. Consequently, in addition to maintaining optimal temperature, it is advisable to store the apples under appropriate humidity conditions.

In another study, a vapor compression refrigeration plant using two different working fluids, R22 and its substitute R417A, was experimentally investigated by Apreo and Renno [10]. The plant is commonly used in commercially available cold stores for preserving foodstuff. Through the experimental analysis, the research team assessed and compared the energetic performances of R22 and R417A. The evaluation was based on various parameters, including the coefficient of performance, exergetic efficiency, exergy destroyed in different plant components, and other variables that characterize the overall performance of the refrigeration system.

Evans et al. [11] conducted an assessment of various methods to reduce energy consumption in food cold stores. They found that many cost-effective improvements, such as enhanced door protection, optimized defrost cycles, control settings, and equipment repairs, could significantly reduce energy usage. In large cold stores (with a capacity greater than 100 m3), these improvements were particularly effective, offering quick payback times. However, in small stores, the options for energy savings were limited, and the payback times were less realistic. By optimizing store usage, repairing existing equipment, and retrofitting

energy-efficient equipment, potential energy savings ranging from 8 % to 72 % were identified. These improvements often yielded short payback times of less than 1 year.

A temperature-controlled cold room kept at 4-6°C was used to store olives in research by Plasquy et al. [12] that found it might postpone further processing and ripening of the olives by up to 4 weeks. It has been observed that by storing the olives until they're processed for oil extraction, it has improved the oil quality. So, the cold room proved its point in prolonging the storage life of olives and in increasing the quality of the olive oil.

2. MATERIALS AND METHOD

2.1. Insulation and Construction Materials

Before determining the total heat transfer coefficient, it is necessary to ascertain the thickness of the structures and the types and thicknesses of insulation materials.

This study used Bloksan companies' expanded polystyrene (EPS) thermo brick, or carbon-reinforced styrofoam, to construct the interior and external walls. The primary feature that sets apart this thermobrick from conventional bricks in the industry is its integration of EPS insulation panels measuring 45 mm in thickness, strategically placed in regions where air gaps commonly occur.

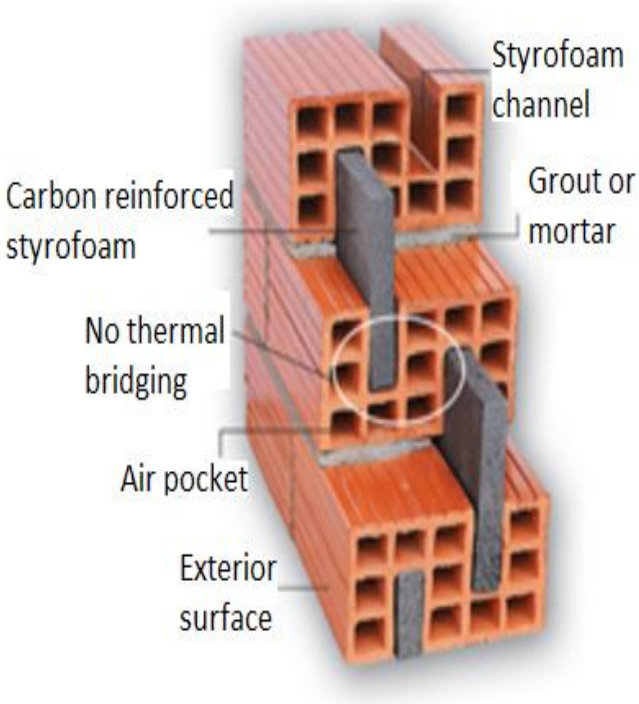

Figure 2. Carbon-reinforced styrofoam thermobrick [13]

As seen in Figure 2, this design modification reduces heat permeability, thereby enhancing the thermal insulation properties of the brick. The third brick in Bloksan's product line features a 45 mm styrofoam, which offers the highest level of thermal insulation or possesses the greatest thickness of insulation material. By employing this procedure, the utilization of additional insulation material becomes unnecessary. The brick's transmission coefficient is 0.095 kcal/mh°C, according to Bloksan's catalog. The brick's dimensions are also provided as 240x240x135 mm [13].

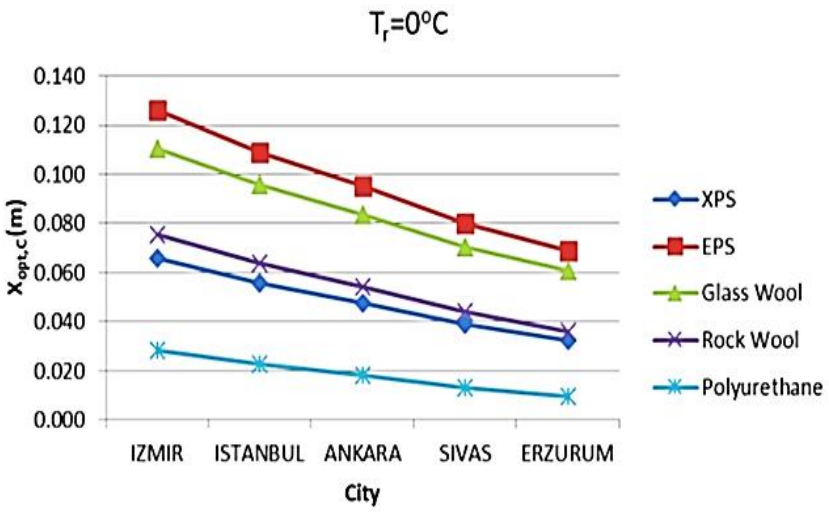

Figure 3. Optimum insulation type and thickness for Ankara province [14]

According to Kürekci's study from 2020 [14], as depicted in Figure 3, the ideal insulation thickness for EPS, XPS and Polyurethane were 95, 54 and 18 mm respectively at 0°C in Ankara province. The determination was made based on electricity and insulation cost factors, considering the specific EPS insulation type and an ambient temperature of 0°C for Ankara province.

As per Özkol's work [15], for storing a product at 0°C in a warm and sunny environment, it is recommended to utilize polyurethane insulation with a minimum thickness of 75 mm. Based on this information, the insulation material selected for this study is EPS, with a thickness of 75 mm.

In order to keep the walls from degrading, coarse plaster was applied to the interior and exterior surfaces of this wall, and the thermal conductivity coefficient of the material is 0.595 kcal/mh°C, according to Ertem's study [16]. To sum it up, the ultimate configuration of the walls consists of the following layers, arranged from the exterior to the interior: a 20 mm exterior plaster, a 240 mm layer of thermobrick, a 75 mm polyurethane layer, and finally, a 20 mm rough plaster. The depiction of the wall has been generated utilizing a CAD software to enhance the visual representation of the arrangement, as shown in Figure 4.

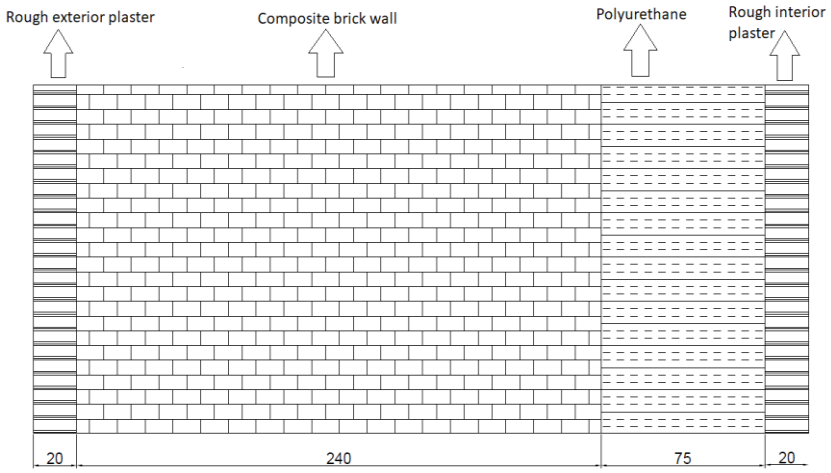

Figure 4. CAD sketch of the walls

The EPS material mentioned above exhibits a porous structure because of its production process, which enhances its ability to either allow passage or retain water vapor and moisture. Extruded polystyrene (XPS) is an alternative insulation material derived from the same base material but manufactured using a different technique. In contrast to expanded polystyrene (EPS), this material exhibits a denser structure with a smaller pore size. Hence, it exhibits greater resistance to external influences and exhibits reduced moisture permeability [17].

Subsequently, XPS was utilized in the flooring to ensure that the intended flooring or the floor insulation would not crack at a weight of more than 25 tons. The heat transfer coefficient has been reported as 0.027 kcal/mh°C. The foundation comprises 150 mm of gravel (1.29 kcal/mh°C). The slab was made of low-density concrete with a thickness of 100 mm, also known as lean concrete. Its heat transmission coefficient was documented as 0.149 kcal/mh°C according to Özkol. In addition, a layer of 50 mm XPS and a layer of 100 mm reinforced concrete were applied once more. The final step was to apply a layer of 25 mm rough plaster with a thermal conductivity of 0.595 kcal/mh°C, followed by a layer of 5 mm mosaic tiles with a thermal conductivity of 1.29 kcal/mh°C [15,18].

The roof of the cold room was constructed using composite polyurethane roof panels from Yazkar Company. A panel with 80 mm thickness was chosen, and its heat transfer coefficient is 0.019 kcal/mh°C [17]. The inner and outer edges of the doors are constructed with a 2 mm AISI 304 stainless steel sheet (12.9 kcal/mh°C) [20] and 100 mm of polyurethane in the middle.

To find the heat gain resulting from infiltration, it is necessary to obtain the dry and wet bulb temperatures of the designated study province. Arslanyan and Zengin's 2017 study in Ankara [21] served as the reference for the wet and dry bulb temperatures. The wet bulb temperature values in Table 1 will be used to calculate the heat gain by infiltration in subsection 2.3.

Table 1. Wet bulb temperatures for Ankara [21]

No	Temperature Lower Limit (°C)	Temperature Upper Limit (°C)	Number of Days
1	-10	-5	5
2	-5	0	20
3	0	5	44
4	5	10	50
5	10	15	94
6	15	20	111
7	20	25	41

Table 2. Dry bulb temperatures for Ankara [21]

No	Temperature Lower Limit (°C)	Temperature Upper Limit (°C)	Number of Days
1	-10	-5	1
2	-5	0	16
3	0	5	42
4	5	10	33
5	10	15	43
6	15	20	78
7	20	25	62
8	25	30	51
9	30	35	39

The highest temperature was recorded at 35 °C, according to Arslanyan and Zengin [21]. In this study, the maximum outside temperature was established to be 35°C, as per Table 2 since it is the absolute highest temperature.

The optimum storage conditions for apples were considered to be 0°C temperature and 90 % relative humidity based on the work of Koyuncu and Eren [8]. Certain conditions were established following the determination of building materials and thermometer temperatures for the cold room design. The conditions and calculations were guided by Özkol's book titled "Applied Cooling Technique" [15]. The facility's walls have been defined as light in color, and its entrance is oriented toward the north. Based on [15], it has been determined that the configuration of the roof will be flat and light in color as well [8,15].

Following the establishment of these parameters, the cold storage's area allocation was calculated in units using the space that would be covered by the pallets and crates that would be utilized to store 25 tons of apples. The pallet was selected as the ISO standard Europalet. The pallet has a load-carrying capacity of 1500 kg. The arrangement consists of four rows stacked vertically, allowing for the placement of eight crates measuring 400x300x240 mm on a pallet with dimensions of 1200x800x144 mm. Thus, a pallet contains 32 crates. For this palette, the dimensions of the GP-22 case from Gülolu Plastik were found to be adequate [22]. This case has a load-carrying capacity of 16 kg. As a result, an estimated total of 49 pallets were utilized, with three of these pallets being stacked to accommodate the storage of 25 tons of apples. Considering the forklift's lifting distance and calculating the entire height as 3312 mm, the warehouse's height was determined to be 3.5 m. The pallets are organized in dual rows along the warehouse's walls, with a 200 mm gap between the wall and each pallet as well as between adjacent pallets. The dimensions of the warehouse were measured at 5400 x 9200 mm. 2.5 meters have been allocated to allow the forklift to maneuver unrestrictedly between the pallets. Upon the inclusion of the office and engine room within the architectural plan, the overall dimensions of the building will amount to 5400 x 13200 x 3500 mm, as seen in Figure 5.

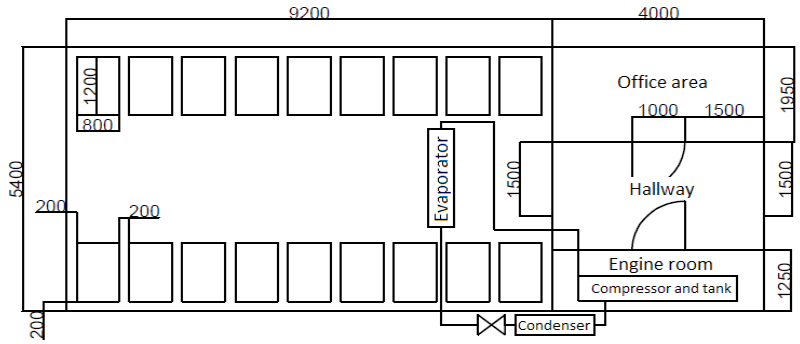

Figure 5. CAD sketch of the cold room

As shown in Figure 5, the facilities' doors were chosen to be 1500 mm wide so that the forklifts could move in and out freely. As for the forklift, the SXV-CB 10 model was chosen from STILL-ARSER. The maximum lifting capacity of this forklift is 1 ton, and it can raise its forks to a height of 5380 mm [23].

2.2. Heat Gain by Transmission

Once the area allocation for the cold store was determined, the heat transfer coefficients of the walls, floor, ceiling, and doors were subsequently computed. The formula used to calculate the total heat transfer coefficient (K) is as follows:

$$K = \frac{1}{\frac{1}{a_{inside}} + \sum_{k=1}^{n} K = \frac{l_n}{\lambda_n} + \frac{1}{a_{outside}}} \quad (1)$$

Here, 'α' denotes the surface transmission coefficient or the heat transmission coefficient of the medium. The symbols 'l' and 'λ' represent the material's thickness and heat transmission coefficient, respectively. After applying the prescribed formula, the resultant value for the overall heat transfer coefficient, denoted as 'K', is determined [24].

The adjacent volume temperatures and the solar radiation impact values are needed to calculate the heat gained via transmission using these subsequently acquired data. To address this matter, it is recommended to refer to Table VII-9 as presented by Özkol [15]. Given the hot climate and the decision to construct the cold storage facility on soil flooring, a temperature of 25°C has been selected. To determine the heat gained from the office area of the warehouse, the non-climatized volumes for typical utilization are within the range of 35–5, specifically 30°C. The temperature figure of 35 + 10 = 45°C is finally used to calculate the heat gained from the engine room. The transmission value is subsequently determined using the

equation below [15].

$$Q = K * A * \Delta T \quad (2)$$

2.3. Heat Gain by Infiltration

In the next step, the heat gain from infiltration will be determined. To perform this, the enthalpies for both indoor and outdoor environments were obtained from the psychometric diagram under the given conditions. The following equation was used to evaluate infiltration [15]:

$$Q_i = ACH * V * \rho_{air} * (h_i - h_o) \quad (3)$$

ACH, which stands for air exchanges per hour, refers to the measurement of the number of times the air within a given space is replaced with fresh air in one hour. The variable 'V' denotes the volume of the room, 'ρ_{air}' denotes the density of the air, and 'h' denotes the internal and external enthalpy values [25].

2.4. Heat Gain from the Products

As per the work of Özkol [15], apples undergoing storage exhibit a heat emission phenomenon during the ripening process. The phenomenon is referred to as the biological process of ripening and respiration heat, which occurs due to the loss of moisture in fresh fruits [26].

Table VII-13 in Özkol's book [15] was consulted to determine the average amount of ripening-respiratory heat released by an apple per day, which is 207.5 kcal/day. The following formula was then used to determine the heat gain from the products:

$$Q_{resp} = m * c_{resp} \quad (4)$$

The variable 'm' represents the mass of the apple, measured in tons, while 'c_{resp}' denotes the daily heat generated by the apple.

Due to the disparity between the temperatures of externally sourced products and the cold storage facility, a thermal energy transfer will occur, resulting in a net heat gain. Based on the data in Table VII-10 of Özkol's publication, an apple's freezing point is recorded as -1.1°C. In the present study, apples are subjected to a storage temperature of 0°C. Consequently, the thermal energy required to raise the temperature of apples to a level above the freezing point prior to freezing is determined to be 0.88 kcal/kg°C. Assuming that apples are in a cooling state, the following cooling load calculation was made [15]:

$$Q_c = m * c_a * \Delta T \quad (5)$$

'm' stands for the mass of the apple as measured in kilograms; 'c_a' is the apple's warming temperature before freezing; and 'ΔT' is the temperature difference between the outside and the warehouse.

Furthermore, it is essential to consider that transporting these apples from external sources will involve using pallets and crates, which may contribute to an increase in heat gain. So, another calculation should be made using the same formula to determine this amount.

2.5 Heat Gain from People

The cold room work assignment entails the presence of a single forklift operator, two warehouse workers, one technician, and one engineer. Their daily working hours in this environment are set at seven hours. Upon examination of Table VII-14 [15], it is observed that there was a heat gain of 235 kcal/h per individual at a temperature of 0°C. The calculation of this gain can be determined by utilizing the following formula:

$$Q_h = c_h * n * t \quad (6)$$

The variable 'c_h' indicates the amount of heat acquired from individuals, 'n' denotes the number of individuals engaged in work, and 't' signifies the duration of their work.

2.6 Heat Gain from Lighting, Forklifts, and Other Devices

A certain quantity of heat will be gained through forklifts, lighting, and other electrical equipment. The light source was a set of 14-100 W Essential E27 bulbs from Phillips. Every 10 m^2 of space will have one light bulb installed. The lights will be on for 8 hours each day. The heat gain from these bulbs can be calculated by using the following equation:

$$Q_l = A * P * c_l * t \quad (7)$$

The variables in this formula can be explained as follows: 'A' stands for the cold room ceiling area; 'P' for the luminaire power; 'c_l' for the lamp specific heat; and 't' for the operating duration.

An electric forklift is desirable, as was previously stated. As a result, the forklift's electric motor will also generate heat. The typical efficiency of electric motors is 90 %. In other words, some energy will undergo friction and become heat energy, radiating outward as heat gain [27]. According to its brochure, this forklift has a 1450 W motor; therefore, if we assume that it will operate for 7 hours per day, then:

$$Q_f = t * P * 0.1 \quad (8)$$

In this equation, 't' stands for run time and 'P' for power.

When figuring the heat gain of other devices, As the apple ripens, it will emit 10 % more ethylene gas into the atmosphere. Frigo Block's ethylene absorber has been placed to eliminate this gas from the environment. The device has a motor of 1 kW, and its operation will result in heat gain [28].

The NUH ATM 3000 ultrasonic humidification system from Frigo Block was also selected to ensure the environment is at ideal humidity levels. Using ultrasonic sound waves, the device turns liquid water into vapor, humidifying the surrounding air. This humidifier has a power output of 340 W, which will also result in heat gain [29].

2.7 Heat Gain from the Evaporator

Once all the heat gains above have been combined, the overall cooling load equals 41.67 kW. After incorporating a 10 % increase to account for the heat gain from the evaporator and other previously unaccounted heat gains, the measured value was determined to be 45.83 kW. Calculations of the evaporator's actual heat output will be made in subsection *2.10,* and the results will be shown in the results section.

2.8 Selection of the Evaporator

For evaporator selection, there are several measures to be taken. These include the temperature difference between the room and the evaporation temperature, the relative humidity level, and the refrigerant type.

The room temperature-evaporation temperature differential is taken from the Applied Cooling Technique book [15]. For fresh fruits, 6.5°C is obtained from Table V-2 [15] using the specified room temperature (0°C) and relative humidity (90 %) values.

See Table V-3 [15] to determine the temperature differential associated with room evaporation based on relative humidity. For 90 % relative humidity, the temperature difference is 5.6°C. The optimal evaporation temperature for this humidity level is 0-5.6 = -5.6°C. As stated in the note under Table V-2 [15], if the temperature of the coil surface is assumed to be approximately 2.5–5.6 °C (-3.1°C), then 0-(-3.1) = 3.1°C is taken into consideration as the evaporation temperature since it is lower than the maximum temperature difference (5.6°C).

The evaporator or coil's surface will have the lowest temperature in a cooled volume. As a result, in high-humidity warehouses, the evaporator's surface will freeze. Defrosting must be done [13] to prevent this freezing. In the next stages of the process, it will be determined when to apply defrost and how much electricity is needed.

The most common refrigerant for use in vapor compression refrigeration systems is R507A, which is an azeotropic mixture of 50:50 by mass composed of R125 and R134A. It has relatively little environmental impact and is in the A1 security class due to its ODP of 0 and its GWP of 3900 [28]. In the study by Arora and Kaushik [30], R507A demonstrated better overall COP and exergy efficiency. R507A was chosen as the refrigerant in this study based on the findings of Arora and Kaushik [28].

The SC2 evaporator standard will be acceptable in the current room conditions at an evaporation temperature of -3.1°C and a cooling load of 45.89 kW. The lamella spacing is 7 mm, and the maximum temperature differential, denoted by ΔT, is -8.

The PSE 50.31.6 device from Frigo Block was chosen as the best option for meeting these criteria, and its specifications can be seen in Figure 6. One unit has a cooling capacity of 26.3 kW. Therefore, two evaporators, whose combined cooling capacity is 52.6 kW, will be adequate to chill the cold store proposed in the study.

PSE - Ø500

Lamel Aralığı Fin Spacing	Model Model	Kapasite Capacity				Yüzey Alanı Surface Area	Boru Hacmi Tube Volume	Hava Debisi Airflow Rate	Fanlar / Fans					Elektrikli Defrost Electric Defrost			Boyutlar Dimensions						Giriş Bağlantısı Çapı Inlet Diameter	Çıkış Bağlantısı Çapı Outlet Diameter
		Soğuk Oda Cold Room		Donmuş Oda Frozen Room					Gerilim Voltage	Adet Piece	Çap Diameter	Güç Power	Akım Current	E1 Batarya Coil	E2 Batarya Coil	E2 Drenaj Tavası Drip Tray	L	K	H	A	A1	F		
		SC1 T_E=0°C DT1=10K	SC2 T_E=-8°C DT1=8K	SC3 T_E=-25°C DT1=7K	SC4 T_E=-31°C DT1=6K																			
mm		kW	kW	kW	kW	m²	L	m³/h	V / ~ / Hz	n	mm	W	A	W	W	W	mm	mm	mm	mm	mm	mm	inch	inch
6	PSE 50.11.6	12,90	8,70	6,90	-	32,90	9,30	6370	230V/1-/50Hz	1	500	710	3,10	9x225	10x225	2x225	1140	630	822	780	-	465	5/8"	7/8"
	PSE 50.12.6	15,00	10,10	7,80	-	43,70	12,00	5840	230V/1-/50Hz	1	500	710	3,10	9x225	10x225	2x225	1140	700	822	780	-	534	5/8"	7/8"
	PSE 50.21.6	25,90	17,50	14,00	-	65,70	18,50	12740	230V/1-/50Hz	2	500	1420	6,20	9x400	10x400	2x400	1890	630	822	1530	-	465	7/8"	1 1/8"
	PSE 50.22.6	30,30	20,40	15,80	-	87,60	24,70	11680	230V/1-/50Hz	2	500	1420	6,20	9x400	10x400	2x400	1890	700	822	750	780	534	7/8"	1 3/8"
	PSE 50.31.6	38,90	26,30	21,00	-	98,60	27,80	19100	230V/1-/50Hz	3	500	2130	9,30	9x600	10x600	2x600	2640	630	822	750	780	465	7/8"	1 3/8"
	PSE 50.32.6	44,90	30,50	24,30	-	131,50	37,10	17520	230V/1-/50Hz	3	500	2130	9,30	9x600	10x600	2x600	2640	700	822	750	780	534	1 1/8"	1 5/8"
	PSE 50.41.6	52,00	35,10	28,10	-	131,50	37,10	25470	230V/1-/50Hz	4	500	2840	12,40	9x800	10x800	2x800	3390	630	822	750	780	465	1 1/8"	1 5/8"
	PSE 50.42.6	60,80	41,10	32,00	-	175,30	49,40	23380	230V/1-/50Hz	4	500	2840	12,40	9x800	10x800	2x800	3390	700	822	750	780	534	1 1/8"	1 5/8"

Figure 6. Specifications of Frigo Block's Evaporators [31]

This evaporator features three fans with a combined power of 2130 W and a 500 mm fan diameter. It has an airflow of 19100m^3/h. The E2 defrost battery has an output of 6120 W.

2.9 Actual Heat Gain from the Evaporator

A small amount of heat gain from the evaporator's motor and fans will be released into the atmosphere in addition to the cooling load value calculated in the preceding sections. Consult Table VII-15 [15] to determine this. The operational period of the evaporator is considered 23 hours and is computed using the formula below after defrosting for 15 minutes four times each day [15]:

$$Q_{evap} = n_{fan} * P * t * 930 \quad (9)$$

In this equation, 'n_{fan}' represents the number of fans, 'P' for fan power, 't' for daily operation time, and '930' for the correcting factor.

The total heat gain can finally be determined once the defrost temperature is calculated. Using the following formula, the defrosting heat gain can be computed:

$$Q_{def} = n_{evap} * P * t * F \quad (10)$$

The term 'n_{evap}' refers to the number of evaporators, 'P' to the evaporator's horsepower, 't' to its activity time, and 'F' to the defrost factor. For electric defrost, this value can be interpreted as '0.5'.

2.10 Selection of the Compressor

The temperature at which the refrigerant condenses should be 10 to 20 degrees Celsius above the air inlet temperature, according to what Özkol stated in his book [15]. Then, using a psychometric diagram and the following parameters: 52.6 kW cooling capacity, 0°C evaporation, and 35 + 10°C condensation temperature, the enthalpy values of the R507A refrigerant should be calculated to determine the compressor capacity. It is possible to figure out the powers of the compressor, condenser, and evaporator using the enthalpy calculations made here. Next, a COP value, also known as a coefficient of performance, can be determined. The COP number serves as a measure of the refrigeration cycles' effectiveness. Removing heat from a medium is the goal of refrigeration cycles, and doing so requires a net power input. The COP can therefore be stated as follows in [25]:

$$COP_R = \frac{Energy\ out}{Energy\ in} \quad (11)$$

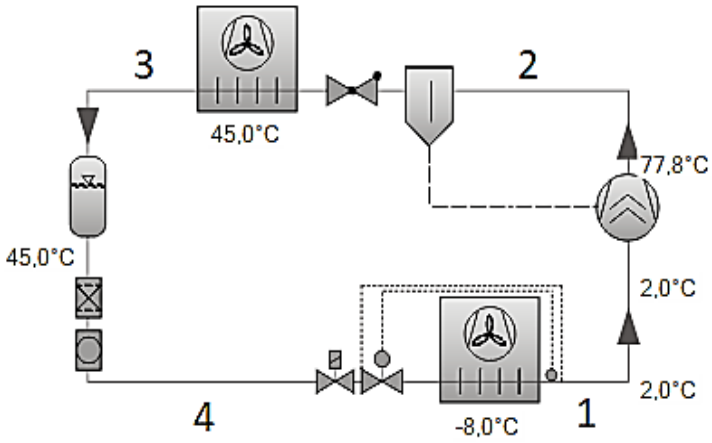

Figure 7. Diagram of a vapor compression cycle [32]

Using the EES tool (Engineering Equation Solver), several R507A refrigerant enthalpy values were found based on the diagram in Figure 7. These enthalpy data allowed for the calculation of the compressor's power and COP. The stages of the vapor compression refrigeration cycle can be stated as follows [25]:

1-2: Isentropic compression occurs in the compressor while the pressure increases.

2-3: Heat transfer from the condenser to the surroundings at constant pressure.

3–4: Lowering the fluid's pressure inside the throttling valve (constant enthalpy)

4-1: Heat transmission to the evaporator fluid while the pressure is constant.

The enthalpy values obtained in the EES software, and the formulas used are given below:

$$Q_{evap} = \dot{m} * (h_1 - h_4) \quad (12)$$

$$W_{comp} = \dot{m} * (h_2 - h_1) \quad (13)$$

$$Q_{cond} = \dot{m} * (h_2 - h_3) \quad (14)$$

The variable '$\dot{m}$' in this equation represents the refrigerant flow rate of the evaporator, and its unit is kg/s. Since the evaporator's cooling capacity is known, equation 11 may be used to determine the flow rate value. Then, a COP value may be calculated using the compressor's power and the condenser's heat capacity:

$$COP = \frac{Q_{evap}}{W_{comp}} \quad (15)$$

A condenser and compressor must be chosen to complete the cooling system. Bitzer's [30] web-based selection guide served as the basis for these decisions. The application starts by picking the preferred compressor type. Özkol [15] asserts that vapor compression refrigeration cycles typically employ semi-hermetic or open-type compressors. In this study, a semi-hermetic screw compressor was preferred. Following input of the refrigerant type, cooling capacity value, refrigerant evaporation temperature, and condensation temperature, the compressor with model number HSK5353-35-40P is recommended. This compressor has a cooling capacity of 54.8 kW, 29.6 kW of power input, 2003 kg/h of flow rate, and 77.4 °C of gas outlet temperature. Additionally, the condenser capacity was found to be 84.3 kW.

3. RESULTS

In this section, the results obtained through the utilization of the equations provided in the materials and methods section will be presented.

Using Equation 1, the overall heat transfer coefficient was calculated. Table 3 lists the total heat transmission coefficients determined by the thickness and heat transfer coefficients of the building components:

Table 3. Total heat transfer coefficients of the building components

Component	K ($kcal/mh°C$)
Inside wall	0.1372
Outside wall	0.1389
Slab	0.2872
Roof	0.2241
Door	0.1666

Then a transmission heat gain value was determined using, through Eq. 2, these total heat transfer coefficient values. The chambers' transmission value was determined to be 47890 kcal/day, equivalent to 2319 W. Subsequently, substituting the matters in subsection 2.3 into Eq. 3, the heat gain of infiltration was calculated to be 14241 kcal/day, or 689 W. Next, using the values given in subsection 2.4 and Eq. 4. the ripening-respiratory temperature of 25 tons of apples was determined to be 251 W. As for the heat gained from the products, upon substituting the given values in subsection 2.4 into Eq 5., the resulting calculation yields a value of 32083 kcal/hour, which can be equivalently expressed as 37287 W. Upon recalculation using Eq. 5, it is determined that 150 W of heat will be gained from the crates. In contrast, the pallets will yield 365 W. The amount of heat gained by people was estimated to be using Eq 6., 8225 kcal/day, which is equivalent to 398 W (subsec. 2.5). The heat gained by the lighting equals 33 W using Eq. 7. (subsec. 2.6). heat gained by the forklifts equals 42 W using Eq 8. The 1 kW motor of the ethylene absorber will result in a heat gain of 100 W, and the humidifier will generate 34 W of heat. The evaporator's actual heat gain equals 8875 W utilizing Eq 9 (subsec 2.9). Then, a 6120 W of heat gain will result from four 15-minute daily thaw cycles (Eq 10). After calculating all the heat gain values transmitted to the cold room, the total heat acquired may be computed. The sum of all heat gains was calculated to be 60.89 kW, as shown in the table below.

Table 4. Total heat gain.

The type of heat gained	Heat gain (W)
Heat gain by transmission	2319
Infiltration	698
Products	38098
People	398
Lighting, forklifts and other	209
Evaporator (10 % increase)	4172
Subtotal	**45894**
Evaporator (actual)	8875
Defrost	6120
Total	**60889**

With the help of EES software, the enthalpy values were calculated and are shown in the table below.

Table 5. Enthalpy values found in the EES software.

No	Enthalpy (kJ/kg)
1	363
2	394
3	268
4	268

After calculating these enthalpy values, the power output of the compressor, the heat capacity of the condenser, the flow rate of the refrigerant, and finally a COP value was calculated utilizing the Equations 12, 13, 14, and 15 the values shown below were found.

Table 6. Flow rate, power, and COP values found in the EES software.

$\dot{m}$ (kg/s)	0.28
W_{comp} (kW)	8.49
COP	3.1

4. CONCLUSION

The necessity to preserve fresh fruit in the best possible circumstances is rising due to the agriculture industry's continued expansion. These fruits need to be kept in optimal temperature and humidity conditions to be preserved with the least amount of mass loss. This study has attempted to address this issue in the best possible manner. The cooling room's space allocation and the necessary number of pallets and boxes were determined using the calculations performed in this study. Additionally, the equipment that would be employed, including the compressor, condenser, evaporator, and refrigerant, was chosen. The thermobricks that were chosen in this study proved to be quite efficient in terms of thermal bridging. In future studies, different construction and insulation materials may be preferred, such as autoclaved aerated concrete bricks, celcon blocks, rock wool, glass wool, etc. Also, with the advancement of refrigeration technology, a different study can be done with the discovery of better refrigerants. Compared to other values in the literature, the study's 3.1 COP value can be considered quite a good result. The research findings have the potential to revolutionize the way perishable agricultural commodities are handled, stored, and transported. They can lead to enhanced food security, reduced food waste, increased economic opportunities, and improved sustainability in the agriculture and food sector. In details, by maintaining optimal humidity and temperature conditions, the cold room design could help increase the availability of apples in the market throughout the year. It would also reduce spoilage and wastage, contributing to more efficient supply chains and lower food waste. Also by reducing post-harvest losses and extending the shelf life of apples, the agricultural industry could experience economic benefits. Farmers would have access to more stable and profitable markets, leading to potential growth and development in the agricultural sector. Finally the research could pave the way for advancements in refrigeration technology specific to cold room designs for other agricultural commodities. The knowledge gained from this study could be adapted and applied to other fruits and vegetables, expanding the scope of efficient storage and transportation in the food industry.

Funding

There are no financial interests in this study.

Declaration of Competing Interest

There is no conflict of interest in this study.

References

[1] ASHRAE Committee, 2018. ASHRAE Handbook: Refrigeration

[2] Hosseini, B., Namazian, A., 2012. An Overview of Iranian Ice Repositories An Example of Traditional Indigenous Architecture, METU Journal of the Faculty of Architecture, 29:2, 223-234.

[3] Gantz, C., 2015. Refrigeration: A History.

[4] Giunta, C. J., 2006. Thomas Midgley, Jr., and the Invention of Chlorofluorocarbon Refrigerants: It ain't Necessarily so, Bulletin for the History of Chemistry 31(2):66-74.

[5] Altun, Ö., Aslantaş, K., Sökmen, E., 2020. Eskişehir İlinde R744 Soğutucu Akışkanlı İki Buharlaştırıcılı Bir Soğuk Hava Deposu Tasarımı, Soğutma Dünyası, 23:88, 50-57.

[6] Calm, J. M., 2008. The Next Generation of Refrigerants—Historical Review, Considerations, and Outlook, Ecolibrium Nov:24-33.

[7] Benhadid-Dib, S., Benzaoui, A., 2012. Refrigerants and Their Environmental Impact Substitution of Hydro Chlorofluorocarbon HCFC and HFC Hydro Fluorocarbon. Search for an Adequate Refrigerant, Energy Procedia, 18, 807-816.

[8] Koyuncu, M.A., Eren, İ., 2005. Bazı Elma Çeşitlerinin Soğukta Depolanma Koşullarının Belirlenmesi, ADÜ Ziraat Fakültesi Dergisi, 2(1):45-52.

[9] Kedd, F., West, C., 1937. Recent Advances in the Work on Refrigerated Gas-Storage of Fruit, Journal of Pomology and Horticultural Science, 14:4, 299-316.

[10] C. Aprea, C. Renno., 2004. Experimental comparison of R22 with R417A performance in a vapour compression refrigeration plant subjected to a cold store, Journal of Energy Conversion and Management, 4, 1807-1819.

[11] J.A. Evans, E.C. Hammond, A.J. Gigiel, A.M. Fostera, L. Reinholdt, K. Fikiin, C. Zilio., 2014. Assessment of methods to reduce the energy consumption of food cold stores, Journal of Applied Thermal Engineering, 62, 697-705.

[12] Plasquy, E., Martos, J. M. G., Florido, M. C., Sola-Guirado, R. R., Martín, J. F. G., 2021. Cold Storage and Tempeature Management of Olive Fruit: The Impact on Fruit Physiology and Olive Oil Quality-A Review, Processes, 9, 1-34.

[13] Bloksan, Styroporlu Termo Yalıtım Tuğlaları, https://bloksan.com.tr/portfolio/bt-19-20-24styroporlu-termo-yalitim-tuglalari-2/, 08.04.2023.

[14] Kürekci, N. A., 2020. Optimum Insulation Thickness for Cold Storage Walls: A Case Study for Turkey, Journal of Thermal Engineering, 6(5), 873-887, Yıldız Technical University Press.

[15] Özkol, N., 1999. Uygulamalı Soğutma Tekniği, Makine Mühendisleri Odası, 115.

[16] Ertem, S., 2006. Konut Dışı Yapılarda İklimlendirme Santrallerinin Tasarımı, İstanbul Teknik Üniversitesi, Fen Bilimleri Enstitüsü, Yüksek Lisans Tezi.

[17] Amir, A. H., Alibaba, H. Z., 2018. Comparison between Heat Conductivity of EPS and XPS, International Journal of Recent Research in Civil and Mechanical Engineering, 4(2):24-31.

[18] Daşdemir, A., 2014. Farklı Yalıtım Malzemesi ve Yakıt Türüne Bağlı Olarak Optimum Yalıtım Kalınlığının ve Enerji Tasarrufunun Tespiti, Makine Mühendisliği Odası, Tesisat Mühendisliği Dergisi, 139, 5-13.

[19] Yazkar, Soğuk Oda Çatı Panelleri, http://sogukoda.yazkar.com.tr/urunlerimiz/soguk-oda-cati-panelleri.html, 08.04.2023.

[20] Blackwell, B. F., Gill, W., Dowding, K. J., Voth, T. E., 2000. Determination of Thermal Conductivity of 304 Stainless Steel Using Parameter Estimation Techniques, Proceedings of NHTC '00 34th National Heat Transfer Conference Pittsburgh, Pennsylvania.

[21] Arslanyan, T., Zengin, G., 2017. Hibrit Tip Kapalı Çevrim Soğutma Kulelerinin Teknik İncelemesi, Makine Mühendisleri Odası, 13. Ulusal Tesisat Mühendisliği Kongresi, İzmir.

[22] Güloğlu Plastik, One Way Kasalar, https://guloglu.com.tr/one-way-kasalar/, 09.06.2023.

[23] STILL ARSER, Elektrili Forklift, https://www.still-arser.com.tr/araclar/yeni-araclar/elektrikli-forklift/sxv-cb-10.html, 09.06.2023.

[24] Çengel, Y. A., 2002, Heat Transfer: A Practical Approach, 2nd edition, Mcgraw-Hill, New York, USA.

[25] Çengel, Y. A., Boles, M. A., Kanoğlu, M., 2023. Thermodynamics: An Engineering Approach, 10th edition, McGraw-Hill, New York, USA.

[26] Becker, B. R., Fricke, B. A., 2002. Transpiration and Respiration of Fruits and Vegetables, University of Missouri-Kansas City, Mechanical and Aerospace Engineering Department, Enviromental Science Paper.

[27] De Almeida, A.T., Ferreira F.J., Fong, J. A. C., 2010. Standarts for Efficieny of Electric Motors, Industry Applications Magazine, 17(1), 12-19.

[28] Frigo Block, Etilen Alma Cihazı, https://www.frigoblock.com.tr/etilen-alma-cihazi.php, 09.06.2023.

[29] Frigo Block, Ultrasonik Nemlendirici, https://www.frigoblock.com.tr/ultrasonik-nemlendirici.php, 09.06.2023.

[30] Arora, A., Kaushik, S. C., 2008. Theoretical Analysis of a Vapour Compression Refrigeration System with R502, R404A and R507A, International Journal of Refrigeration, 31, 998-1005.

[31] Frigo Block, Standard Evaporatörler, https://www.frigoblock.com.tr/standart-evaporatorler.php, 09.06.2023.

[32] Bitzer, Web Software, https://www.bitzer.de/websoftware/Default.aspx, 08.07.2023.